Green Reports

Ariviyal Publishing

Research Article

DOI: 10.36686/Ariviyal.GR.2020.01.01.002

Green Rep., 2020, 1(1), 8-15.

Green Synthesis of Silver Nanoparticles for Antimicrobial Activity

P. Venkatesan,[a] A. Selvamani,[b] R. Balasubramanian,[c] C.M. Babu,[d] S. Poovarasan,[b] V.V. Srinivasan,[e] A. Shakila Parveen,[c] P. Thirukumaran,[c] B. Sundaravel*[f] and V. Ramkumar*[b]

[a]*Department of Biotechnology, University of Madras, Chennai - 600025, Tamil Nadu, India.*
[b]*CSIR-Central Leather Research Institute, Chennai - 600020, Tamil Nadu, India.*
[c]*Department of Chemical Engineering, Yeungnam University, South Korea.*
[d]*Department of Chemical and Biomolecular Engineering, National university of Singapore, Singapore - 117585.*
[e]*Department of Chemistry, National Institute of Technology, Tiruchirappalli - 620015, Tamil Nadu, India.*
[f]*Department of Chemistry, Kalasalingam Academy of Research and Education, Krishnankoil, Tamil Nadu - 626126, India.*

***Corresponding author E-mail address**: sundar.chem.bala@gmail.com (B. Sundaravel); srirams27@gmail.com (V. Ramkumar)

ISSN: 2582-6239

Crossref

Publication details
Received: 1st November 2019
Revised: 2nd December 2019
Accepted: 2nd January 2020
Published: 6th January 2020

Abstract: Silver nano-particles (AgNPs) were prepared by biosynthesis method and the prepared AgNPs were tested towards anti-microbial activity. Powder X-ray diffraction (XRD), scanning electron microscope (SEM), transmission electron microscope (TEM), ultraviolet–visible spectroscopy (UV-Visible) and Fourier-transform infrared spectroscopy (FT-IR) analysis were used to test the resultant AgNPs. TEM and SEM results revealed the formation of spherical shape of AgNPs. The powder XRD result implies the average particle size of AgNPs was 18 nm. The anti-microbial activity of the AgNPs was tested against several gram negative and gram positive bacteria. The anti-bacterial activity of ampicillin was found to be increased when it is companied with the present AgNPs. The investigation of antimicrobial effect against human pathogens revealed the greater efficacy of AgNPs.

Keywords: Silver nanoparticles; Bio-synthesis; T. tetrahele; Anti-microbial activity; TEM; XRD

1. Introduction

In recent days, nanotechnology plays a virtual role in various fields such as energy, biomedical, environmental science, optics, catalysis, and biotechnology etc.[1-4] Indeed, the shape and morphology of the nanomaterials are much important in respect of the application. Hence, researchers have widely focused in developing such nanomaterials including AgNPs for a wide range of applications in the fields of bio-labeling, sensors, antimicrobial filters, and bactericidal activity. AgNPs is proved to be the most active candidate for the bactericidal activity against gram-positive and gram-negative bacteria. The AgNPs also have significant potential for a wide range of applications such as catalysis, magnetic recording media, opto-electronic materials, magnetic fluids, composite materials, fuel cells, pigments and sensors.[1-3] Nanotechnology provides the ability to engineer the properties of materials by controlling their size and shape. Nanomaterials have emerged as an alternative in chemical and pharmaceutical industry due to their outstanding properties including optical, magnetic, catalytic, optoelectronic and thermal properties.[5,6] This has driven research towards the potential use of nanomaterials. So far, various methods have been developed for the synthesis of AgNPs and the resultant AgNPs were utilized for the potential applications such as catalysis, magnetic recording media, opto-electronic materials, magnetic fluids, composite materials, fuel cells, pigments and sensors.[5-9]

Metal nanoparticles (MNPs) prepared via eco-friendly methods have been proven to be effective in controlling and suppressing the bacterial growth.[10] Among various metal nanoparticles, AgNPs has gained a peculiar characteristic of acting as an antimicrobial agent, as it releases biologically active Ag+ ions upon ionization, even in its solid state. The AgNPs coated polyurethane foam acted as an antibacterial water filter.[9] AgNPs synthesized using Aspergillus niger could efficiently inhibit various pathogenic organisms, including bacteria and fungi.[10] The green synthesis of AgNPs using plant extracts of Aloe vera, Portulaca Oleracea and Cynodon Dactylon, the AgNPs can be synthesized at low cost and also demonstrated the antibacterial effect of the AgNPs.[11] Hence, it could be observed that, AgNPs can be synthesized using a bio-system and also could be used as an effective antibacterial agent. Recently, AgNPs with different size, morphology and stability was synthesized by conventional physical and chemical methods, by altering the preparation method, solvent, reducing agent and temperature.[12,13] But most of them are regarded as hazardous, expensive and have low productivity.[14] In order to overcome this issue, several researchers adopted biological systems to synthesize nanoparticles.[15]

The fungus mediated biological route for the synthesis of barium titanate nanoparticles,[16] the magnetic behavior of the nanoparticles

can be studied with the help of biological systems which opens up new prospects in the magnetic nanomaterials.[17] The AgNPs size of 40 nm was synthesized using culture supernatant of Klebsiella Pneumonia.[18] The extacelluar biosynthesis of AgNPs using fungi Penicillium Fellutanum obtained from Mangrove root soil, the enzyme protein of nitrate reductase might be involved in the formation of AgNPs.[19] The synthesized AgNPs showed significant antibacterial action on both the Gram classes of bacteria.[20,21] the AgNPs were synthesized using fungus Trichoderma viride for the extracellular biosynthesis, and the result showed that combination of antibiotics with AgNPs have better antimicrobial effects.

The absorption of Au+ ions by Chlorella Vulgaris from aqueous solutions and formation of metallic Au bound algae which opened the new pathway for nanomaterial synthesis.[22] Besides the production of NPs, algae are also being explored for determining its nutritional value, efficacy in bio-diesel improvement as well as its vast potential for therapeutic application.[23] AgNPs are synthesized from bacteria, fungi, yeast and various parts of plants, such as flowers, leaves and fruits. Hence, in this present work discloses the synthesis of AgNPs via biological method using Tetraselmis tetrahele (T. tetrahele) algal as an extract for the first time and the synthesized material have been tested for antimicrobial studies against human pathogens.

2. Materials and Methods

2.1. Chemicals and Microorganism

All chemicals and media components are of analytical grade and purchased from Sigma-Aldrich, and used as received. The algae Tetraselmis-Tetrahele was used as the source microalgae and the strain was obtained from Central Marine Fisheries Research Institute (CMFRI), Tuticorin and maintained at National Institute of Ocean Technology (NIOT).

2.2. Biomass Production

In the typical procedure, the algae were grown in a general enriched sea water medium (f/2 medium). In a 1000 mL standard measuring flask 950 mL of filtered natural sea water was taken. To the above solution, 1 mL of 0.882 M sodium nitrate solution, 1 mL of 0.0362 M sodium dihydrogen monohydrate solution and 1 mL of aqueous solution containing less than 1 ppm of Fe^{3+}, Cu^{2+}, Mo^{6+}, Zn^{2+}, Co^{2+} and Mn^{2+} ions along with sodium salt of EDTA were added. Finally, 1 mL of aqueous solution containing trace amount of vitamin B1, H and B12 were also added to the flask. The final volume was made up to 1000 mL and used as a medium (Guillard f/2 medium) for algae growth. In a 500 mL Erlenmeyer flask 250 mL of the prepared Guillard f/2 medium and algae strain was taken. The culture was exposed to a light level of 1500 lux at 24±2°C. After 72 h, the algal cells were extracted by centrifugation at 5000 rpm for 15 minutes. The medium components adhered (if any) to the biomass was removed by washing with sterile double distilled water thoroughly. The biomass obtained was subjected to freeze drying to remove the water content and thick pellet of biomass as shown in fig. 1 is obtained after complete dehydration. Fig. 1 shows the freeze dried biomass of Tetraselmis tetrahele.

Fig. 1. Freeze dried biomass of Tetraselmis tetrahele.

Fig. 2. Crude extract of Tetraselmistetrahele.

2.3. Biosynthesis of AgNPs

In a Scott Duron bottle containing 100 mL of sterile double distilled water and 50 mg of freeze dried biomass powder were suspended and subjected to sonication for 60 minutes at 25 °C. Then the extract was filtered through Whatmann-1 filter paper and then the filtrate was stored at 4°C for further use. The crude extract is shown in Fig. 2.

In an autoclave, silver nitrate (1 mmol) suspended in 100 mL of the cell filtrate obtained from the biomass (shown above) was subjected to 15 psi pressure at 121°C for 15 minutes. In another autoclave, the reaction was carried out without the precursor of Ag. As the reaction proceeds, change in color was observed for the reaction mixture containing silver ions while the color of the reaction mixture with no silver ions remains the same as always. The appearance of brownish black color solution suggested the formation of AgNPs. Ag ion is a powerful oxidizing agent which interacts with the metabolites present in the algal biomass and gets reduced to metallic AgNPs. Hence it may be inferred that the redox reaction is accompanied by electron transfer from the biomass to the Ag ions present in the solution. After completion of the reaction, the AgNPs was separated by centrifugation at 15,000 rpm for 10 minutes. After centrifugation the supernatant liquid was discarded and the residue was washed with double distilled water to remove free ions, the loosely bound and uncoordinated biological molecules adhered to the product.

2.4. Growth Assessment

The cell count analysis was carried out using Haemocytometer (Neubauer). The algal samples collected and preserved in Lugol's

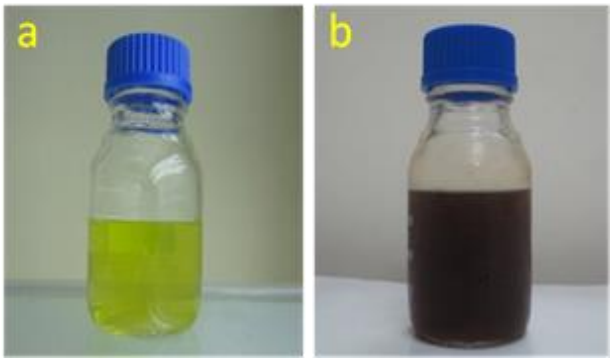

Fig. 3. Reaction mixture before (a) and after (b) the formation of AgNPs.

Fig. 4. Triplicates of Tetraselmistetrahele.

iodine solution was diluted with the culture medium and counting was done under light microscope (40x objective, Carl Zeiss, model Axioskop 2 (HAL 100 MC 80DX, Germany) and the number of cells were calculated by using equation (1).

$$\text{No. of cells} = \frac{\text{Total cells counted}}{\text{No. of squares used X Dilution factor}} \times 10^4 \quad (1)$$

For initial and final biomass determination, 5 ml aliquots of biomass was rapidly centrifuged for 5 minutes and the pellet was re-suspended in distilled water and filtered through a pre-weighed, pre-dried glass fiber filter paper (Millipore GF/C 47 mm, pore size 1.2 µm) and washed thrice in distilled water. During the filtration, the vacuum pressure differentials were maintained at 35 to 55 mm Hg. The filter papers with algal cells were dried at 70°C in an oven to constant weight and cooled down to room temperature in a vacuum desiccator prior to weighing and biomass was calculated using equation (2)

$$\text{Cell Dry Weight} = \frac{(A-B) \times 1000}{\text{Sample Volume}}\ g/L \quad (2)$$

Where A = weight of filter + residue before ignition (mg), and B = weight of filter + residue after ignition (mg).

2.5. Characterization

The crystalline nature of purified bio-synthesized AgNPs was analyzed by powder X-ray diffraction technique using Bruker D8-Advanced XRD Instrument, the sample was placed into the sample holder operated at a voltage of 40 kV and a current of 30 mA with Cu Kα radiation. The optical density (OD) of the culture fluid was measured at 540 nm using double beam UV-Vis spectrophotometer (SHIMADZU). The solution was scanned in the range of 200-600 nm using a quartz cuvette with distilled water as the reference. The purified solution of silver nanoparticles was subjected to Fourier Transform Infrared Spectroscopy Analysis (FTIR) to identify the functional group present in the synthesized nanoparticles with help of FTIR spectrometer (Perkin Elmer). SEM studies were carried out to determine the morphology of Ag nanoparticles using Hitachi S-3400N electron microscope operated between 0.3 to 30 kV and equipped for a magnification of 30000X.TEM images were recorded using High resolution transmission electron microscope JEOL, JEM 2100 which was operated at 200 kV.

2.6. Antimicrobial Activity Tests

The antimicrobial assays were carried out on various pathogenic strains by standard disc diffusion method and colony counting method. Luria Bertani (LB) broth/agar medium was used to cultivate pathogens. Fresh overnight culture of inoculums (100µL) of each culture was spread on to Muller Hinton Agar (MHA) plates. Sterile paper disc of 5 mm diameter containing same concentration of (10µg/µL) Ag nanoparticles, algal extract and ampicillin antibiotics were placed in each plate. Silver nanoparticles and standard antibiotic containing discs were used for determining the synergetic activity of nanopaticles. For the colony count assay, different concentrations of AgNPs ranging from 100-500 µL were injected on the plate. The plates were incubated at 37°C for overnight. Next day the inhibition zones around the discs and no of colonies were measured. In order to understand the synergistic effect of AgNPs with antibiotic, the combination of these AgNPs with antibiotics was investigated against gram-positive and gram-negative bacteria using the disk diffusion method. The plates were incubated at 37°C for overnight. Next day the inhibition zones around the discs and no of colonies were measured. The diameters of the inhibition zone (mm) around the antibiotic disk with and without AgNPs against test strains were measured.

3. Results and Discussions

3.1. Algal Growth Analysis

The growth of micro algae (T.tetrhele) was studied throughout the growth period by measuring the optical density (OD) of the culture medium, determining the cell count and calculating the dry weight of the bio mass. The biomass was grown in three different Erlenmeyer flasks as shown in Fig. 4.

The OD pattern is shown in Table 1 and Fig. 5. Initially the OD values were noticed to be not changed significantly because the micro-algae is adapting to the environmental conditions. After 3 days of duration, the OD values changed rapidly and reached the maximum value on 10th day. This duration where the intense growth of algal biomass appeared was known as exponential phase. The OD value shows almost similar values from day 11 to 13 which meant that the algal growth reached maximum and this growth period was known as the stationary phase. After day 13 a decrease in OD value was observed due to the microalgae cell destruction.

Table 1. Tetraselmis Tetrahele Growth assessment

Number of Days	OD_{540}	Number of cells X 10^6	Biomass Weight (g/L)
1	0.02	7.22	0.52
2	0.03	16.67	
3	0.04	25.0	
4	0.11	47.2	
5	0.18	75.0	0.96
6	0.20	90.0	
7	0.22	98.3	
8	0.26	107.2	
9	0.31	141.6	
10	0.34	166.1	1.34
11	0.36	175.0	
12	0.37	179.4	
13	0.37	142.2	
14	0.34	117.2	
15	0.32	92.7	0.74

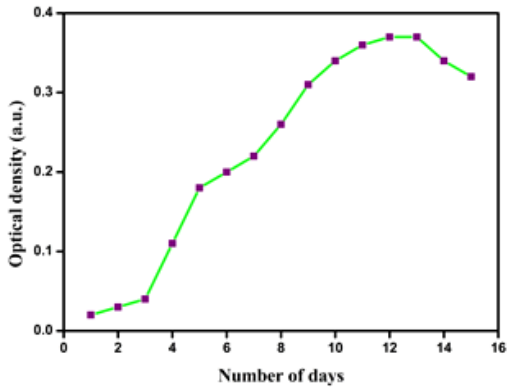

Fig. 5. Cell density analysis of Tetraselmistetrahele.

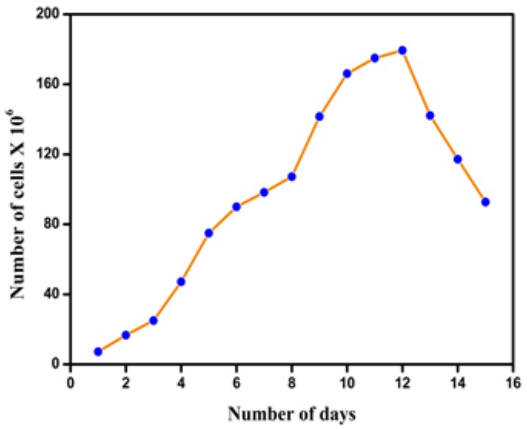

Fig. 6. Cell count analysis of Tetraselmistetrahele.

This OD measurement was also supported by cell count analysis which is presented in Table 1 and Fig. 6. These results showed that the number of algal cells observed on day 12 was maximum and began to decline afterwards.

The dry weight analysis of biomass is shown in Fig. 7. A portion of the culture medium (5 ml) was utilized for calculating the dry weight of the biomass. The biomass samples collected on day 1, 5, 10 and 15 showed a gradual increase and reached maximum on day 10. Hence, it may be inferred that the microalgae attained a maximum growth on day 10, sustained till day 12 and cell death occurred from day 13.

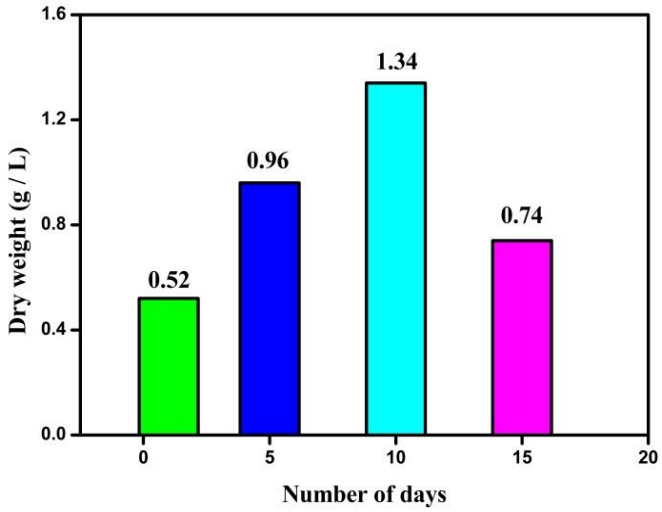

Fig. 7. Dry weight analysis of Tetraselmistetrahele.

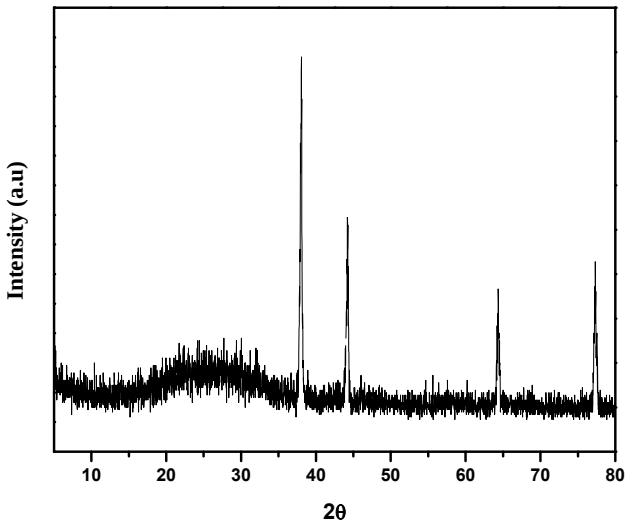

Fig. 8. XRD patterns of biosynthesized Ag nanoparticles.

3.2. Characterization of Biosynthesized Ag-Nanoparticles

3.2.1. Powder X-ray Diffraction (XRD)

The diffraction pattern of biosynthesized silver nanoparticles was shown in Fig. 8. The XRD showed a Bragg reflection close to 2θ value 38° corresponding to (111) lattice plane of face-centered cubic (FCC) structure of silver.[5] XRD pattern thus clearly shows that the silver nanoparticles are crystalline in nature. In addition to this peak, there are also some unassigned peaks, which suggest that the crystallization of bio-organic phase occurs on the surface of the silver nanoparticles.[24] Crystallite size of AgNPs was calculated from the full width at half maximum (FWHM) of the (111) peak using the Scherrer's formula showed average particles size of 18 nm.

3.2.2. UV-Vis Spectroscopy

The UV-visible spectrum of AgNPs was shown in Fig. 9. The AgNPs showed a strong absorbance peak centered at 446 nm, which indicates the formation of AgNPs extracellularly. Presence of additional peak was also noticed at 270 nm, which is attributed to aromatic amino acids of proteins. This band aroused by bio-

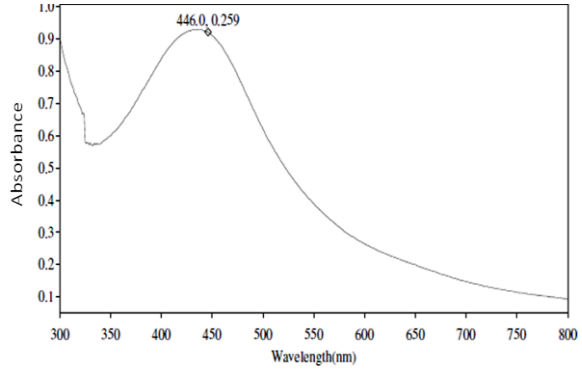

Fig. 9. UV-Vis spectrum of AgNPs.

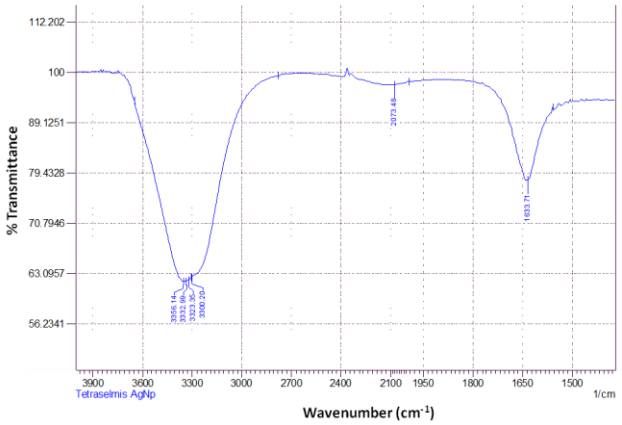

Fig. 10. FT-IR spectrum of AgNPs.

synthesized AgNPs may be due to the electronic excitation of tryptophan and tyrosine in proteins.[21]

3.2.3. FT-IR Analysis

FT-IR spectrum of extracellular biosynthesized AgNPs is shown in Fig. 10. The spectrum shows bands at 1634, 3300, 3323, 3333, 3356 cm^{-1}, respectively, and confirms the presence of N-H, C-H and O-H groups present in the algal. The band at 3356 cm^{-1} corresponds to O-H streching, and the bands at 3333, 3323, 3300 cm^{-1} correspond to C-H strechings of alkynes.[25] The presence of band at 1633 cm^{-1} is assigned to a primary amine (N-H) group. The position of these bands were close to those reported for native proteins.[26] FT-IR results indicate that secondary structures of proteins were not affected as a consequence of reaction with Ag+ ions or binding with AgNPs. This evidence suggests that the release of extracellular protein molecules could possibly perform function for the formation and stabilization of silver nanoparticles in aqueous medium.

3.2.4. SEM Analysis

The SEM micrographs of AgNPs are shown in Fig. 11a & b. The SEM images revealed that the AgNPs are spherical in shape but agglomerates together to form an irregular structure. The morphology of AgNPs was predominately spherical and aggregated with larger irregular structure which has no well-defined morphology.[27] The nanoparticles were not in direct contact even within the aggregates, indicating stabilization of the nanoparticles by a capping agent (proteins secreted by algal extracts). The presence of

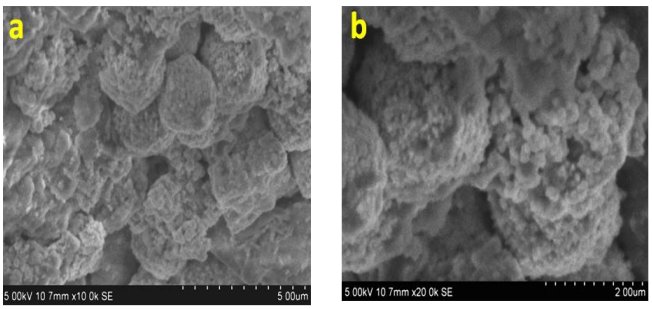

Fig. 11. (a and b) SEM images of Ag nanoparticles.

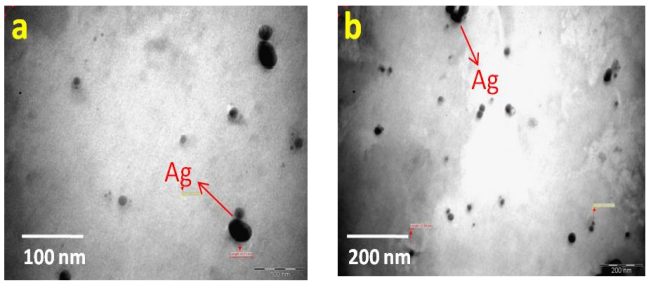

Fig. 12. (a and b) TEM images of Ag nanoparticles.

Table 2. Colony forming unit of micrococcus in different concentrations of silver nanoparticles

S. No	Concentration of AgNPs	(CFU/ml x 10^4)
1	0	1500
2	100	892
3	200	569
4	300	320
5	400	205
6	500	90

secondary materials capping with the silver nanoparticles may be assigned to bio-organic compounds from algal extracts.[28]

3.2.5. TEM analysis

TEM images of bio-synthesized AgNPs are shown in Fig. 12a & b. These micrographs clearly illustrate that AgNPs are spherical in shape in the range of 10-40 nm in size. The reduction of silver metal ions (Ag+) by algal extracts leads to the formation of silver nanoparticles of fairly well defined dimensions.[29,30] The control of shape and size of silver nanoparticles seems to be easy with the use of algal extracts. This analysis further proves that the nanoparticle does not have direct contact even within the aggregates as seen in SEM results.

3.3. Algal Growth Analysis

3.3.1. Colony Counting Test

Fig. 13 and Table 2 illustrate the antibacterial activity of silver nanoparticles. At zero concentration the number of colonies present was around 1500x10^4cfu/ml and found to be decreasing (90x10^4cfu/ml) when the concentration of Ag nanoparticles increases. Thus it showed that increased concentration of AgNPs affects the growth of the microbes.

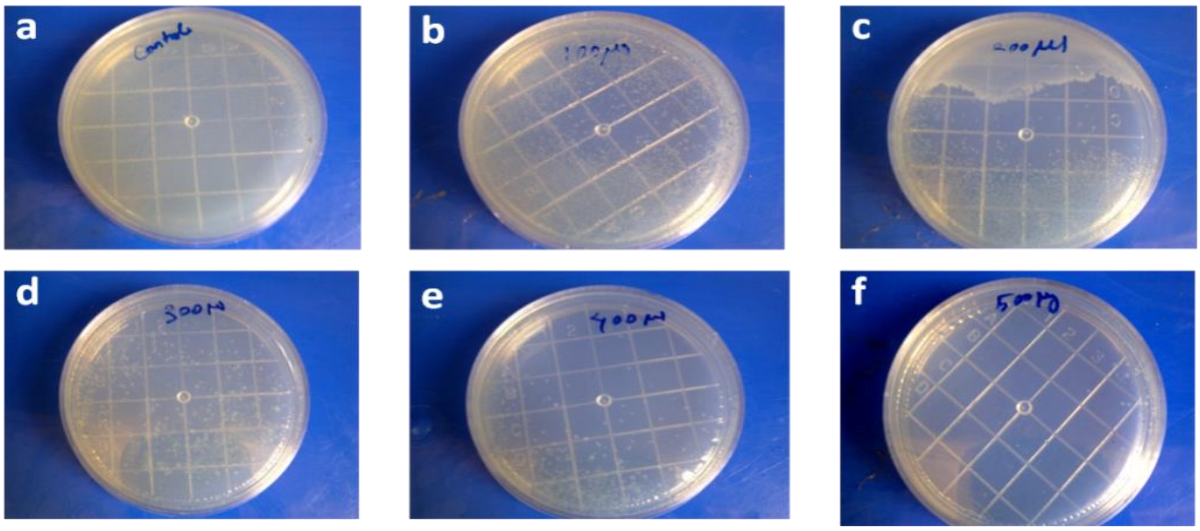

Fig. 13. a-0 µg/µl of AgNPs, b-100 µg/µl of AgNPs, c-200 µg/µl of AgNPs, d-300 µg/µl of AgNPs, e-400 µg/µl of AgNPs and f- 500 µg/µl of AgNPs.

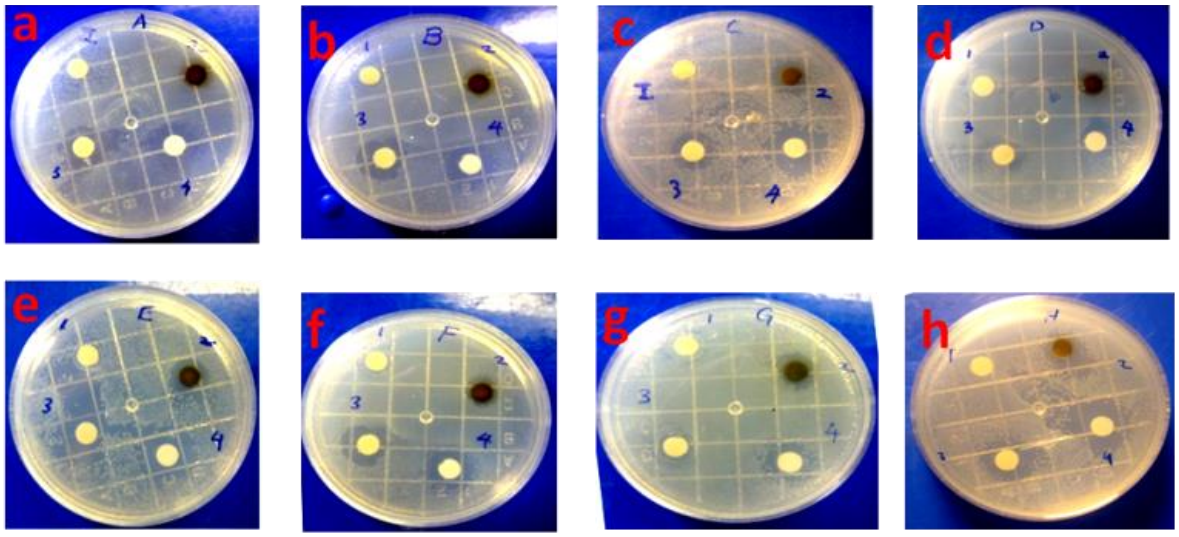

Fig. 14. Zone of inhibition (mm) from disk diffusion performed against pathogen, a- Vibrio cholera, b-Micrococcus luteus, c-Klebsiella pneumonia, d Pseudomonas aeruginosa, e-Staphylococcus aureus, f-E.cloi, g-Streptococcus pneumonia and h-Bacillus subtilis, 1-Algal extract, 2- Silver nitrate, 3- AgNPs, 4-Ampicillin.

Table 3. Zone of Inhibition (mm) from Disk diffusion analysis

Organism	Zone of Inhibition (mm)			
	Algae extract	Silver nitrate	Silver nanoparticle	Antibiotic
A	0	1	8	9
B	0	3	8	11
C	0	1	6	9
D	0	1	5	8
E	0	5	9	12
F	0	2	6	8
G	0	3	6	7
H	0	2	10	11

3.3.2. Disk Diffusion Test

Fig. 14 shows the antimicrobial activity of bio-synthesized AgNPs against different bacteria. As it showed a clear inhibition zone (Table 3), the synthesized silver nanoparticles were equally effective in their activity against pathogens compared to antibiotics. Algal extract was used as negative control while antibiotic and silver nitrate were used as positive control.

3.3.3. Synergistic Effect of Ag Nanoparticles with Antibiotic

The combination of these AgNPs with antibiotics was investigated against gram-positive and gram-negative bacteria using the disk diffusion method (Fig. 15). The diameter of inhibition zone (mm) around antibiotic disk with and without Ag nanoparticles against test strains is shown in Table 4, and these results revealed that antibacterial activity of ampicillin increased in the presence of Ag nanoparticles against test strains. Bacterial proteins and DNA makes preferential sites for silver nanoparticles interaction as they possess sulphur and phosphorus compounds and silver have higher affinity to react with these compounds.

Antibacterial effect of AgNPs obeyed a dual action mechanism of antimicrobial activity, (i.e.) the bactericidal effect of Ag+ and membrane disrupting effect of the polymer subunit.

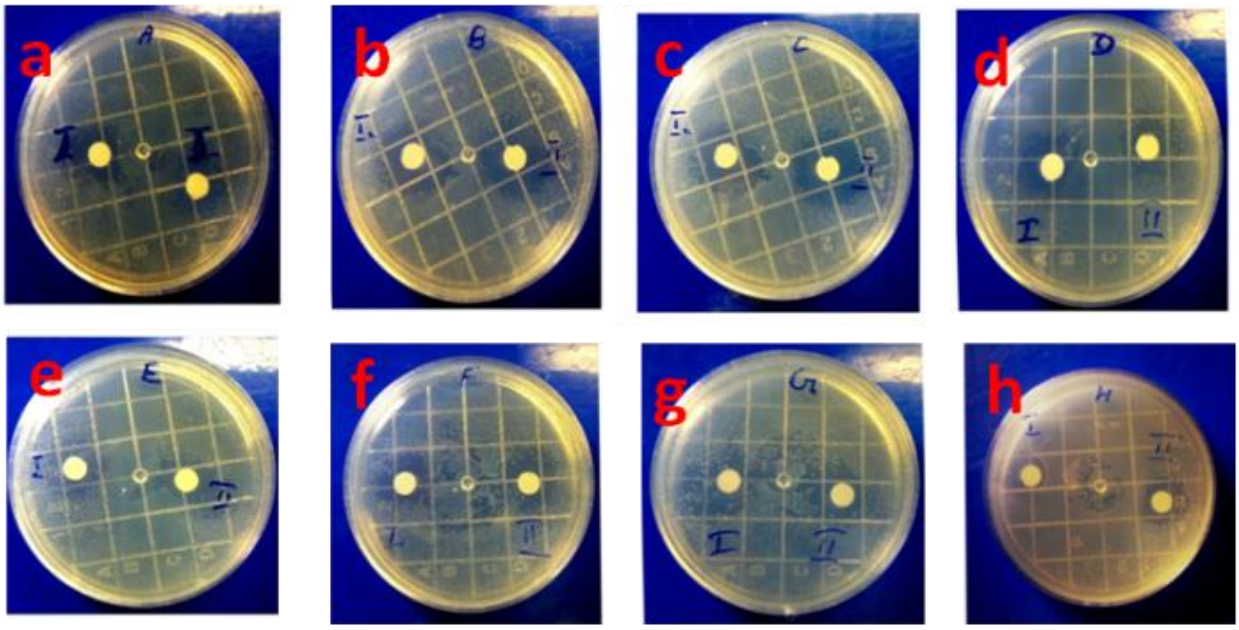

Fig. 15. Synergistic effect of AgNPs with antibiotic performed against pathogens. a-Vibrio cholera, b-Micrococcus luteus, c-Klebsiella pneumonia, d- Pseudomonas aeruginosa, e-Staphylococcus aureus, f-E.cloi, g-Streptococcus pneumonia and h-Bacillus subtilis, I-Antiniotic, II – AgNPs + Antibiotic.

Table 4. Synergistic Effect of Ag nanoparticles with Antibiotic against Human Pathogens

Microorganism	Ampicillin (10 µ g/disk) Zone (mm)		Fold increase % = ((b – a)/a) × 100
	Ampicillin (a)	AgNPs + Ampicillin (b)	
A	9	10	11.11
B	11	15	36.3
C	9	12	33.3
D	8	10	25
E	12	15	25
F	8	11	37.5
G	7	10	42.8
H	11	14	27.2

4. Conclusions

A simple biosynthetic method was developed (as an alternative to chemical and physical method) for the preparation of AgNPs. The resultant AgNPs were characterized by various spectroscopic and microscopic techniques. The T. tetrahele proves to be an important biological component for extracellular biosynthesis of stable AgNPs. An investigation on the antimicrobial effect of bio-synthesized AgNPs against human pathogens reveals high efficacy as a strong antimicrobial agent. This green chemistry approach towards the synthesis of AgNPs has many advantages such as ease with which the process can be scaled up, economic viability and no toxic chemicals used. Uses of such biosynthesized nanoparticles in medical and other applications make the biosynthetic method to be potentially used for the large-scale synthesis of other inorganic nanomaterials.

Acknowledgements

The author P. V would like to thank the DRDO, UGC-DRS and DST-FIST for providing an instrumentation facility in the Department of Biotechnology, University of Madras, Chennai, India. The authors V. R and A. S greatly acknowledge the DST-SERB-NPDF/2017, New Delhi for providing National Post-Doctoral Fellowship (NPDF) to carry out the research work.

Conflicts of Interest

The authors declare no conflict of interest.

References

1 Ramos A.P.; Cruz M.A.; Tovani C.B.; Ciancaglini P. Biomedical Applications of Nanotechnology. *Biophys. Rev.*, 2017, **9**, 79-89. [CrossRef]
2 Day J.K.; Das S.; Mawlong L.G. Nanotechnology and its Importance in Micronutrient Fertilization. *Int. J. Curr. Microbiol. Appl. Sci*., 2018, **7**, 2306-2325. [CrossRef]
3 Singh A.; Prasad S.M. Nanotechnology and its Role in Agro-Ecosystem: A Strategic Perspective. *Int. J. Environ. Sci. Technol.*, 2017, **14**, 2277-2300. [CrossRef]
4 Kholoud M.; Abou E.; Ala E.; Abdulrhman A.W.; Reda A.A. Synthesis and Applications of Silver Nanoparticles. *Arab. J. Chem*., 2010, **3**, 135-140. [CrossRef]
5 Lee S.H.; Jun B.H. Silver Nanoparticles: Synthesis and Application for Nanomedicine. *Int. J. Mol. Sci*., 2019, **20**, 865. [CrossRef]
6 Siddiqi K.S.; Husen A.; Rao R.A. A Review on Biosynthesis of Silver Nanoparticles and their Biocidal Properties. *J. Nanobiotechnol*., 2018, **16**, 14. [CrossRef]
7 Hulkoti N.I.; Taranath T.C. Biosynthesis of Nanoparticles using Microbes—A Review. *Colloids Surf. B: Biointer*., 2014, **121**, 474-483. [CrossRef]
8 Schacht V.; Neumann L.; Sandhi S.; Chen L.; Henning T.; Klar P.; Theophel K.; Schnell S.; Bunge M. Effects of Silver Nanoparticles on Microbial Growth Dynamics. *J. Appl. Microbiol*., 2013, **114**, 25-35. [CrossRef]
9 Jain P.; Pradeep T. Potential of Silver Nanoparticle-Coated Polyurethane Foam as an Antibacterial Water Filter. *Wiley Inter. Sci*., 2005, **90**, 59-63. [CrossRef]

10 Gaikwad S.; Bhosale A. Heterocyclic Corrosion Inhibitors for J55 Steel in a Sweet Corrosive Medium. *Euro. J. Exp. Biol.*, 2012, **2**, 1654-1658. [CrossRef]
11 Tarad A.; Sulaiman A.; Saleh S.; Milton W. Bactericidal Activity of Biosynthesized Silver Nanoparticles against Human Pathogenic Bacteria. *Biotechnol. Biotechnol. Equipment*, 2017, **31**, 411-417. [CrossRef]
12 Xuping S.; Shaojun D; Wang E. One-step Synthesis and Characterization of Polyelectrolyte-Protected Gold Nanoparticles through a Thermal Process. *Polymer*, 2004, **45**, 2181-2184. [CrossRef]
13 WonSik S.; TaeHwan K.; JaeSuk S. Hydrogen & Fuel Cell Technology. *Korean Chem. Eng. Res*., 2004, **42**, 1-9. [CrossRef]
14 Kowshik M.; Ashtaputre S.; Kharrazi S.; Vogel W.; Urban J.; Kulkarni S.K.; Paknikar K.M. Extracellular Synthesis of Silver Nanoparticles by a Silver-Tolerant Yeast Strain MKY3. *Nanotechnology*, 2002, **14**, 95-100. [CrossRef]
15 Xiangqian L.; Huizhong X.; ZheSheng C.; Guofang C. Biosynthesis of Nanoparticles by Microorganisms and Their Applications. *J. Nanomat*., 2011, **2011**, 16 Pages. [CrossRef]
16 Bansal V.; Poddar P.; Ahmad A.; Sastry M. Room-Temperature Biosynthesis of Ferroelectric Barium Titanate Nanoparticles. *J. American Chem. Soc*., 2006, **128**, 11958-11963. [CrossRef]
17 Dickson D. Nanostructured Magnetism in Living Systems. *J. Magn. Magn. Mater*., 1999, **203**, 46-49. [CrossRef]
18 Mokhtari N.; Daneshpajouh S.; Seyedbagheri S. Biological Synthesis of Very Small Silver Nanoparticles by Culture Supernatant of Klebsiella Pneumonia: The Effects of Visible-Light Irradiation and the Liquid Mixing Process. *Mater. Res. Bull*., 2009, **44**, 1415-1421. [CrossRef]
19 Kathiresan K.; Manivannan S.; Nabeel M.A.; Dhivya B. Studies on Silver Nanoparticles Synthesized by a Marine Fungus, *Penicillium fellutanum* Isolated from Coastal Mangrove Sediment. *Colloids Surf. B: Biointer.*, 2009, **71**, 133-137. [CrossRef]
20 Aruna J.; Sashidhar R.; Arunachalam J. Size-Controlled Green Synthesis of Silver Nanoparticles Mediated by Gum Ghatti (*Anogeissus latifolia*) and its Biological Activity. *Org. Medi. Chem. Lett.*, 2012, **2**, 17. [CrossRef]
21 Fayaz A.; Balaji K.; Girilal M.; Yadav R.; Kalaichelvan P.; Venketesan R. Biogenic Synthesis of Silver Nanoparticles and their Synergistic Effect with Antibiotics: A Study Against Gram-Positive and Gram-Negative Bacteria. *Nanomed. Nanotechnol. Biol. Med.*, 2010, **6**, 103-109. [CrossRef]
22 Hosea M.; Greene B.; McPherson R.; Henzl M.; Alexander M.; Darnall D. Accumulation of Elemental Gold on the Alga *Chlorella vulgaris*. *Inorg. Chim. Acta*., 1986, **123**, 161-165. [CrossRef]
23 Tatyana Z.; Natalia B. Prospects for the Therapeutic Application of Sulfated Polysaccharides of Brown Algae in Diseases of the Cardiovascular System: Review. *Pharm. Biol*., 2016, **54**, 3126-3135. [CrossRef]
24 Sathyavathi R.; Krishna M.B.; Rao S.V.; Saritha R.; Rao D.N. Biosynthesis of Silver Nanoparticles Using Coriandrum Sativum Leaf Extract and Their Application in Nonlinear Optics. *Adv. Sci. Lett.*, 2010, **3**, 138-143. [CrossRef]
25 Anja H.; Kathrin B.; Ulf K.; Daniel R.; Markus G. Analysis of Mycosporine-Like Amino Acids in Selected Algae and Cyanobacteria by Hydrophilic Interaction Liquid Chromatography and a Novel MAA from the Red Alga *Catenella repens*. *Mar. Drugs*, 2015, **13**, 6291-6305. [CrossRef]
26 Macdonald I.; Smith W. Orientation of Cytochrome c Adsorbed on a Citrate-Reduced Silver Colloid Surface. *Langmuir*, 1996, **12**, 706-713. [CrossRef]
27 Arputhamani S.; SindhuPriya D.; Joyce N.; Shiny P.; Amitava M.; Natarajan C. Biosynthesis of Silver Nanoparticles using Actinobacterium *Streptomyces Albogriseolus* and its Antibacterial Activity. *Biotechnol. Appl. Biochem*., 2012, **59**, 503-507. [CrossRef]
28 Ahmad A.; Mukherjee P.; Senapati S.; Mandal D.; Khan M.; Kumar R.; Sastry M. Extracellular Biosynthesis of Silver Nanoparticles using the Fungus *Fusarium Oxysporum*. *Colloids Surf. B: Biointer*., 2003, **28**, 313-318. [CrossRef]
29 Ericka R.; Ramon I.; Rosa E.; Ronaldo H.; Judith T.; Claudia I. Synthesis of Silver Nanoparticles using Reducing Agents Obtained from Natural Sources (*Rumex Hymenosepalus* Extracts). *Nanoscale Res. Lett*., 2013, **8**, 318. [CrossRef]
30 Railean-Plugaru V.; Pomastowski P.; Wypij M.; Szultka-Mlynska M.; Rafinska K.; Golinska P.; Dahm H.; Buszewski B. Study of Silver Nanoparticles Synthesized by Acidophilic Strain of Actinobacteria Isolated from the of *Picea Sitchensis* Forest Soil. *J. Appl. Microbiol*., 2016, **120**, 1250-1263. [CrossRef]